Original Article | Cardiovascular Imaging

eISSN 2005-8330
https://doi.org/10.3348/kjr.2020.0107
Korean J Radiol 2020;21(12):1299-1309

Korean Journal of Radiology
KJR

Histological Validation of Cardiovascular Magnetic Resonance T1 Mapping for Assessing the Evolution of Myocardial Injury in Myocardial Infarction: An Experimental Study

Lu Zhang, MS[1]*, Zhi-gang Yang, MD, PhD[2]*, Huayan Xu, MD[1], Meng-xi Yang, MD[2], Rong Xu, MD[1], Lin Chen, MS[1], Ran Sun, MD[3], Tianyu Miao, MD[4], Jichun Zhao, PhD[4], Xiaoyue Zhou, PhD[5], Chuan Fu, MS[6], Yingkun Guo, MD[1]

[1]Department of Radiology, Key Laboratory of Birth Defects and Related Diseases of Women and Children of Ministry of Education, West China Second University Hospital, Sichuan University, Chengdu, China; [2]Department of Radiology, West China Hospital, Sichuan University, Chengdu, China; [3]Key Laboratory of Obstetrics & Gynecology and Pediatric Disease and Birth Defects of Ministry of Education, West China Second University Hospital, Sichuan University, Chengdu, China; [4]Vascular Surgery, West China Hospital, Sichuan University, Chengdu, China; [5]Siemens Healthineers Ltd., Shanghai, China; [6]Department of Radiology, West China Second Hospital, Sichuan University, Chengdu, China

Objective: To determine whether T1 mapping could monitor the dynamic changes of injury in myocardial infarction (MI) and be histologically validated.

Materials and Methods: In 22 pigs, MI was induced by ligating the left anterior descending artery and they underwent serial cardiovascular magnetic resonance examinations with modified Look-Locker inversion T1 mapping and extracellular volume (ECV) computation in acute (within 24 hours, n = 22), subacute (7 days, n = 13), and chronic (3 months, n = 7) phases of MI. Masson's trichrome staining was performed for histological ECV calculation. Myocardial native T1 and ECV were obtained by region of interest measurement in infarcted, peri-infarct, and remote myocardium.

Results: Native T1 and ECV in peri-infarct myocardium differed from remote myocardium in acute (1181 ± 62 ms vs. 1113 ± 64 ms, $p = 0.002$; 24 ± 4% vs. 19 ± 4%, $p = 0.031$) and subacute phases (1264 ± 41 ms vs. 1171 ± 56 ms, $p < 0.001$; 27 ± 4% vs. 22 ± 2%, $p = 0.009$) but not in chronic phase (1157 ± 57 ms vs. 1120 ± 54 ms, $p = 0.934$; 23 ± 2% vs. 20 ± 1%, $p = 0.109$). From acute to chronic MI, infarcted native T1 peaked in subacute phase (1275 ± 63 ms vs. 1637 ± 123 ms vs. 1471 ± 98 ms, $p < 0.001$), while ECV progressively increased with time (35 ± 7% vs. 46 ± 6% vs. 52 ± 4%, $p < 0.001$). Native T1 correlated well with histological findings ($R^2 = 0.65$ to 0.89, all $p < 0.001$) so did ECV ($R^2 = 0.73$ to 0.94, all $p < 0.001$).

Conclusion: T1 mapping allows the quantitative assessment of injury in MI and the noninvasive monitoring of tissue injury evolution, which correlates well with histological findings.

Keywords: *Cardiovascular magnetic resonance; Cardiac; T1 mapping; Myocardial infarction; Histology*

Received: February 11, 2020 **Revised:** April 9, 2020 **Accepted:** April 24, 2020

This work was supported by the National Natural Science Foundation of China (81471721, 81471722, 81641169, 81771887, 81771897, 81901712, and 81971586); the Program for New Century Excellent Talents in University (No. NCET-13-0386); the Program for Young Scholars and Innovative Research Team in Sichuan Province (No. 2017TD0005) of China; the Applied and Fundamental Study of Sichuan Province (No. 2017JY0026) and 1·3·5 project for disciplines of excellence, West China Hospital, Sichuan University (No. ZYGD18013).

*These authors contributed equally to this work.

Corresponding author: Yingkun Guo, MD, Department of Radiology, Key Laboratory of Birth Defects and Related Diseases of Women and Children of Ministry of Education, West China Second University Hospital, Sichuan University, 20# Section 3 South Renmin Road, Chengdu 610041, China.

• E-mail: gykpanda@163.com

INTRODUCTION

Although mortality after myocardial infarction (MI) is on the decline, the subsequent complications remain one of the significant causes of death worldwide (1, 2). Myocardial injury in MI is closely associated with long-term recovery and prognosis (3-5). Therefore, the accurate evaluation of the severity of myocardial damage plays an essential role in cardioprotective therapies and risk stratification. Cardiovascular magnetic resonance (CMR) has currently evolved into a gold standard for tissue characterization and quantification in MI. However, late gadolinium enhancement (LGE) imaging is of limited value to the quantitative assessment of tissue injury in acute MI (6, 7). T1 mapping has been proposed as a promising technique for tissue characterization due to its accurate diagnosis (8-10). It provides complementary information to standard LGE imaging with excellent performance in detecting myocardial edema (11-13) and fibrosis (14-17). Furthermore, several recent studies demonstrated that native T1 mapping and extracellular volume (ECV) maps could quantify the severity of the injury and predict the left ventricular (LV) function recovery or adverse remodeling (8, 18), adding incremental prognostic value over LGE. However, major efforts related to these works are being applied in clinical practice, while further histological validation is still lacking (18). Accordingly, we sought to histologically validate the feasibility of T1 mapping for quantifying the myocardial injury and monitoring its evolution in the MI pig model.

MATERIALS AND METHODS

Experimental Animal

All experimental protocols in this study were approved by the Institutional Animal Care and Use Committees. Twenty-three male Bama mini pigs with an average weight of 8.8 kg were used in this study. The pigs were premedicated with atropine sulfate (Atropine Sulfate Injection, Jieyang Longyang Animal Pharmaceutical Co., Ltd.) (0.05 mg/kg). 10–15 minutes later, anesthesia was induced by intramuscular injection with Zoletil 50 (Virbac) (10–15 mg/kg). Following intubation with an endotracheal tube, an intravenous channel was established in ear vein to sustain anesthesia with continuous propofol (10 mg/mL, Propofol Injectable Emulsion, XiAn Libang Pharmaceutical Co.,Ltd.). MI was induced by left anterior descending artery ligation for 40 minutes via thoracotomy and was confirmed by the elevation of ST segment on electrocardiogram. The wound and the surgical area were wrapped with povidone-iodine disinfectant after sutured. After drying, the wound was coat with dry penicillin powder and wrapped with sterile gauze, which was changed once a day. To prevent infection, penicillin (100000 IU/kg) was administered intramuscularly twice daily for 3–5 days.

Despite efforts of resuscitation, one pig died before CMR scanning. The surviving pig models underwent serial CMR scans in acute (within 24 hours), subacute (7 days), and chronic (3 months) MI after surgery. Following the examinations, the pigs were sacrificed for histological staining on the same day. The experimental procedure is presented in Figure 1.

Cardiovascular Magnetic Resonance Study

The CMR scanning was conducted using a clinical 3T MR scanner (MAGNETOM Skyra, Siemens Healthineers) equipped with an 18-channel receive coil. CMR protocols included cine, T1 mapping, and LGE. The LV function was assessed with a balanced steady-state free precession pulse sequence (echo time [TE] = 1.70 msec; repetition time [TR] = 46.68 msec; flip angle = 34°; slice thickness 5 mm; matrix = 128 x 128 pixels; field of view [FOV] = 130 x 130 mm^2). A modified Look-Locker inversion recovery method was used

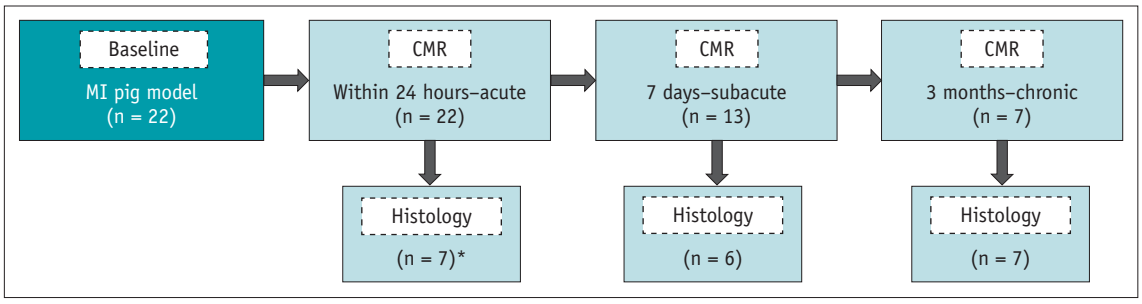

Fig. 1. The following chart shows the different steps from coronary artery occlusion to histological staining. *Two of the 22 pigs were euthanasia for other purposes. CMR = cardiovascular magnetic resonance, MI = myocardial infarction

https://doi.org/10.3348/kjr.2020.0107

Korean Journal of Radiology
KJR

to obtain native T1-maps and post-contrast T1-maps with a 3-3-5 acquisition within one breath-hold's time. Native T1-maps (TE = 1.27 msec; TR = 344.48 msec; flip angle = 35°; slice thickness = 5 mm; matrix = 110 x 192 pixels; FOV = 176 x 150 mm^2) were timed consecutively in three standard short-axis levels (basal, mid, and apical), which were acquired from the middle 3 of 5 parallel short-axis slices spaced equally between the mitral annulus and the LV apical tip. Post-contrast T1-maps (TE = 1.27 msec; TR = 344.48 msec; flip angle = 35°; slice thickness = 5 mm; matrix = 110 x 192 pixels; FOV = 136 x 136 mm^2) were imaged at approximately 15 minutes after intravenous injection of gadolinium at a dose of 0.15 mmol per kg body weight. Breath-hold LGE-imaging was subsequently acquired at 16–20 minutes by using segmented-turbo-FLASH-PSIR (TE = 1.33 msec; TR = 476.60 msec; flip angle = 40°; slice thickness = 5 mm; matrix = 110 x 192 pixels; FOV = 136 x 136 mm^2). Additionally, cine, LGE, and T1 mapping imaging were carried out using a contiguous stack of short-axis slices covering the whole LV for each acquisition. For animals, a breath-hold was acquired during expiration breath-hold mode with a ventilator throughout the CMR examination. At every follow-up stage, comprehensive CMR scans were performed until sacrifice (i.e., animals sacrificed at the chronic stage underwent acute, subacute, and chronic CMR examinations).

Image Analysis

MRI images were analyzed offline using commercially available software (cvi42, Circle Cardiovascular Imaging) (Fig. 2). The basic parameters of LV function were evaluated globally using cine short-axis stack views according to

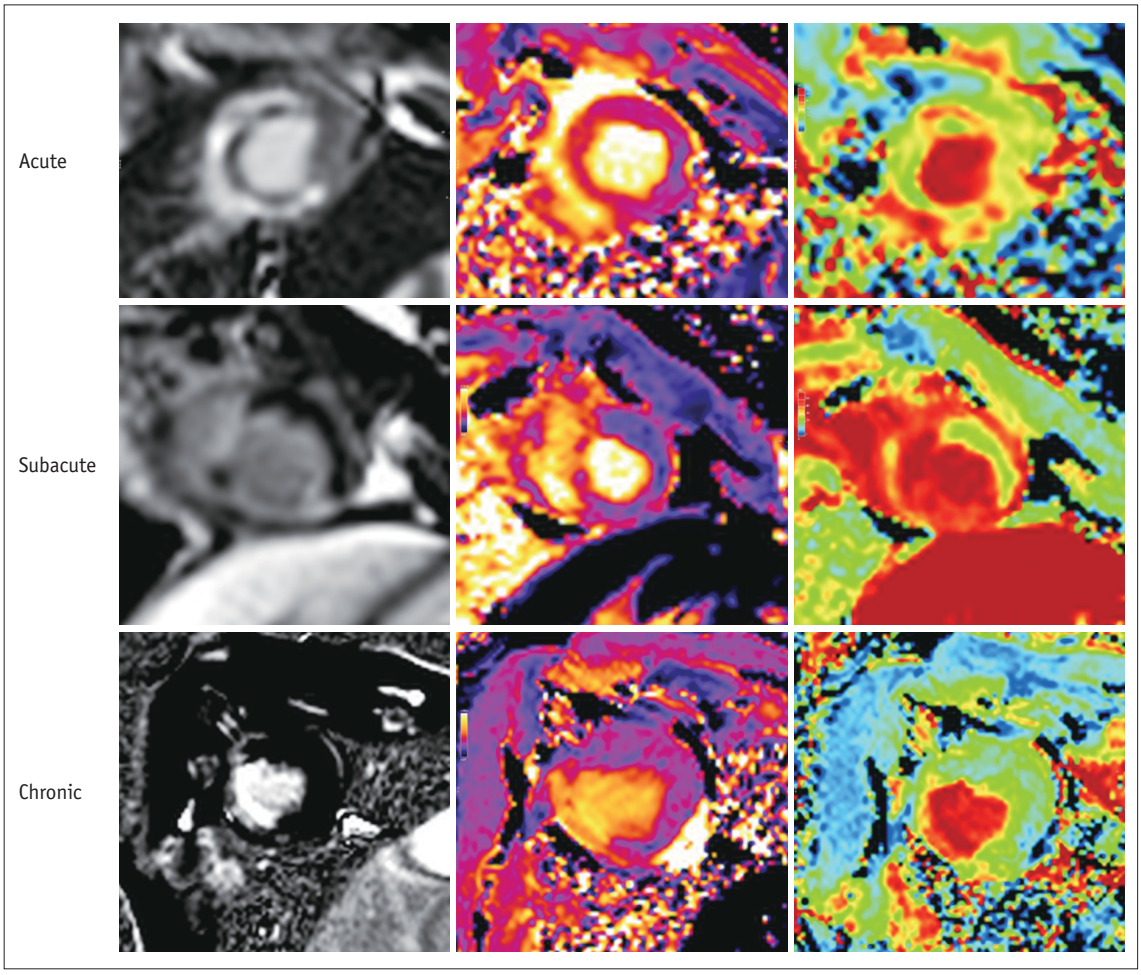

Fig. 2. LGE images (left), native T1 maps (middle), ECV maps (right). The infarcted myocardium was defined using the threshold of 5 standard deviations above the remote myocardial signal intensity. Microvascular obstruction was defined as a hypointense area within the hyperintensity on LGE and included in the measurement of infarct size. The optimal contrast among infarcted, peri-infarcted, and remote myocardium was observed in native T1 and ECV maps in acute and subacute MI but was not significant in the chronic stage. ECV = extracellular volume, LGE = late gadolinium enhancement

https://doi.org/10.3348/kjr.2020.0107

Society for Cardiovascular Magnetic Resonance for reporting of standard post-processing (19). An area of LGE ≥ 5 standard deviations (SD) above remote myocardium (20, 21) was obtained to examine infarct size, expressed as a percentage of total LV mass. Additionally, microvascular obstruction (MVO) was identified as a low-intensity black area in the middle of the hyperintense zone on LGE images and was included in the measurement of LGE infarct with drawing manually.

For the region of interest (ROI)-based T1 mapping measurement, the ROIs were placed in infarcted myocardium (defined as the matching hyperintense area on LGE), peri-infarcted myocardium (defined as the region adjacent to the infarction), and remote myocardium (defined as the area with no LGE and movement dysfunction). To measure ECV, pre- and post-contrast blood T1 times were obtained in additional ROIs manually delineated in the center of the LV cavity (trabeculations or papillary muscles were excluded). ECV was quantified from pre- and post-contrast T1 times according to the established formula (22): ECV fraction = (1 - hematocrit) x ($T1_{myo\ post}$ - $T1_{myo\ pre}$) / ($T1_{blood\ post}$ - $T1_{blood\ pre}$). The ROIs of various regions on pre-contrast images were transposed on the ECV maps with manual and minor correction if needed. The native T1 and ECV of MVO were also derived by ROI-based measurement. For analysis purposes, the characteristics measured with different techniques were confined to the same location, and the delineation of ROIs was performed by the consensus of two radiologists (with three years of experience and with four years of experience).

Histological Analysis

Following CMR examinationss, all pigs were immediately euthanized using potassium chloride. The hearts of pigs were collected and cleaned in saline, and then were left into plastic containers to cool down for approximately 20 minutes at 20 degrees Celsius below zero until solid. The hearts were cut into short-axis slices with a thickness of 5 mm. After fixed and embedding, slices were cut into sections of 5 μm, followed by hematoxylin and eosin and Masson's trichrome staining. Quantitative analysis was performed using Image-Pro Plus 6.0 software (Media Cybernetics). For each sample, 3 visual fields were taken in the infarcted myocardium, 2 on each side of peri-infarcted myocardium (i.e., with approximately 4–6 mm proximal to the infarct) and 1 in the remote myocardium (6). ECV derived by histology was expressed as (extracellular space / total area) x 100, after removing artifacts and perivascular and endocardial fibrous tissue by manually differentiating the extracellular space from viable myocytes with careful consideration. The ECV for each region was averaged in the defined myocardium of each animal.

Statistical Analysis

All statistical data analyses were conducted using SPSS software (v. 17.0 for Windows, SPSS Inc.). The results are expressed as the mean ± SD or median with range, as appropriate. The Shapiro-Wilk test and Leven's test were performed to check normal distribution and homogeneity of variances, respectively. To analyze the changes in all obtained parameters with time, one-way ANOVA or nonparametric tests were utilized. The linear regression was employed to compare native T1 and ECV by CMR versus ECV by histology, respectively. For all comparisons, two-tailed p values < 0.05 were considered statistically significant.

RESULTS

The Baseline Characteristics of the Experimental Study

The baseline characteristics of the experimental study are described in Table 1. Infarct size was significantly decreased from acute to subacute phase (8.4 ± 1.6% vs. 5.8 ± 2.4%, p = 0.017) but showed no difference between subacute and chronic phase (5.8 ± 2.4% vs. 4.0 ± 1.9%, p = 0.317). From acute to chronic phases, the improvements in LV functional parameters were observed as shown in Table 1. The peak creatine kinase release was obviously higher in the acute phase than in the subacute and chronic phases (p = 0.027).

Time Course of Native T1 and ECV in Different Myocardial Regions

The quantitative values of native T1 and ECV derived from CMR are summarized in Table 2. Native T1 of peri-infarct myocardium in the acute phase was significantly higher than that of remote myocardium (p = 0.002), but less than that of infarcted myocardium (p < 0.001) as was ECV (p = 0.031 and p < 0.001, respectively). This trend persisted in the subacute study (all p < 0.05). However, the difference between peri-infarct and remote myocardium disappeared either in native T1 (p = 0.934) or in ECV (p = 0.109) in the chronic setting. Furthermore, the two parameters of infarcted myocardium were still larger than those of remote myocardium in chronic MI (all p < 0.05).

Interestingly, from acute to chronic phases, native T1 of

https://doi.org/10.3348/kjr.2020.0107

Korean Journal of Radiology
KJR

Table 1. Baseline Characteristics of Myocardial Infarction Pigs

	Acute (n = 22)	Subacute (n = 13)	Chronic (n = 7)	*P*
LVEF, %	36.3 ± 15.9	41.2 ± 14.3	56.4 ± 7.5*	0.012
LV EDV, mL	21.1 ± 10.0	16.7 ± 6.5	34.3 ± 13.7*†	0.003
LV ESV, mL	12.7 ± 4.1	9.5 ± 2.2	13.9 ± 4.3	0.062
SV, mL	7.9 ± 5.8	7.4 ± 4.9	19.0 ± 9.5*†	0.001
CO, mL	0.7 (0.4–1.5)	0.7 (0.4–1.3)	1.8 ± 0.8	0.463
LV mass, g	12.4 (9.9–30.0)	13.6 (11.5–14.9)	32.2 ± 8.5*†	0.01
Infarct size, %	8.4 ± 1.6	5.8 ± 2.4*	4.0 ± 1.9*	< 0.001
Troponin I, μg/L	0.075 (0.047–0.113)	< 0.012	< 0.012	-
CK, U/L	1019 ± 444–10590	262 ± 163*	403 ± 247	0.027
CK-MB, μg/L	1.3 ± 0.6–2.6	0.8 ± 0.4	0.7 ± 0.3	0.162
Mb, μg/L	302 ± 222	69.4 (19.9–172.8)	127.1 ± 57.1	0.085
Hct, %	37.2 ± 4.4	35.5 ± 3.8	42.5 ± 4.0*†	0.005

Data are presented as the mean ± standard deviation, or median (interquartile range). *p < 0.05 vs. acute, †p < 0.05 vs. subacute. CK = creatine kinase, CK-MB = creatine kinase-MB, CO = cardiac output, EDV = end-diastolic volume, ESV = end-systolic volume, Hct = hematocrit, LV = left ventricular, LVEF = left ventricle ejection fraction, Mb = myoglobin, SV = stroke volume

Table 2. Dynamic Changes in Myocardial Native T1 and ECV

	Native T1 Time, ms				ECV, %			
	Infarcted	Peri-Infarct	Remote	*P*	Infarcted	Peri-Infarct	Remote	*P*
Acute (n = 22)	1275 ± 63	1181 ± 62*	1113 ± 64*†	< 0.001	35 ± 7	24 ± 4*	19 ± 4*†	< 0.001
Subacute (n = 13)	1637 ± 123	1264 ± 41*	1171 ± 56*†	< 0.001	46 ± 6	27 ± 4*	22 ± 2*†	< 0.001
Chronic (n = 7)	1471 ± 98	1157 ± 57*	1120 ± 54*	< 0.001	52 ± 4	23 ± 2*	20 ± 1*	< 0.001

Data are presented as the mean ± standard deviation. *p < 0.05 vs. acute, †p < 0.05 vs. subacute. ECV = extracellular volume

infarcted myocardium peaked in the subacute phase (acute vs. subacute vs. chronic: 1275 ± 63 ms vs. 1637 ± 123 ms vs. 1471 ± 98 ms, p < 0.001), while a progressive elevation was observed in ECV over 3 months (acute vs. subacute vs. chronic: 35 ± 7% vs. 46 ± 6% vs. 52 ± 4%, p < 0.001). Similar to the trend of native T1 in infarcted myocardium, both native T1 and ECV of peri-infarct myocardium reached peak values in the subacute phase and then decreased in the chronic phase (Fig. 3B, C). Besides, no difference was observed in remote myocardium at all imaging time-points (all p > 0.05).

In the acute phase, 15 out of 22 pigs presented MVO (68.2%). The native T1 of the MVO (1219 ± 49 ms) was higher than that of the remote myocardium (1105 ± 55 ms, p < 0.001) but lower than that of the infarcted myocardium (1282 ± 66 ms, p = 0.03). ECV of the MVO (15 ± 6%) was lower than that of the infarcted myocardium (38 ± 10%, p < 0.001) and had no significant difference compared with the remote myocardium (20 ± 3%, p = 0. 338).

Measurement of ECV Using Histology

In total, 120 microscopy regions from 18 pigs were used in the analysis; two pigs in the chronic phase were excluded because of poor stained. Figure 4 shows the typical histological features of injured myocardium in MI. Damaged tissue following MI evolved from the loss of nuclei, myocardial edema, and inflammatory cell infiltration to the replacement of collagenous fiber. The ECV of peri-infarct myocardium differed from that of remote myocardium in acute (p < 0.001) and subacute MI (p < 0.001) but disappeared in chronic MI (p = 0.668). Furthermore, a longer duration of myocardial ischemia resulted in more serious ECV expansion in the infarcted myocardium (p < 0.001) (Fig. 3A).

Relationship of CMR-Derived Native T1 and ECV with Histological Results

From acute to chronic MI, an excellent correlation was found in the comparison between native T1 and histological ECV (R^2 = 0.65 to 0.89, all p < 0.001) (Fig. 5A-C). Similarly, CMR-measured ECV showed a strong association (R^2 = 0.73 to 0.94, all p < 0.001) (Fig. 5D-F) and close agreement with histological ECV ([acute: bias, 1.4 ± 5.7], [subacute: bias, 1.4 ± 8.2], [chronic: bias, 0.4 ± 9.4]).

DISCUSSION

This study performed a longitudinal assessment of the variation of native T1 and ECV at multiple time points in the

 https://doi.org/10.3348/kjr.2020.0107

MI pig model and conducted a corresponding histological validation. The main findings of our study are that 1) the patterns of the myocardium in native T1 and ECV were different, showing that native T1 reached a peak value in the subacute phase while ECV progressively increased over 3 months post-infarction, and 2) native T1 and ECV could quantify the severity of myocardial damage in MI and were correlated well with histology.

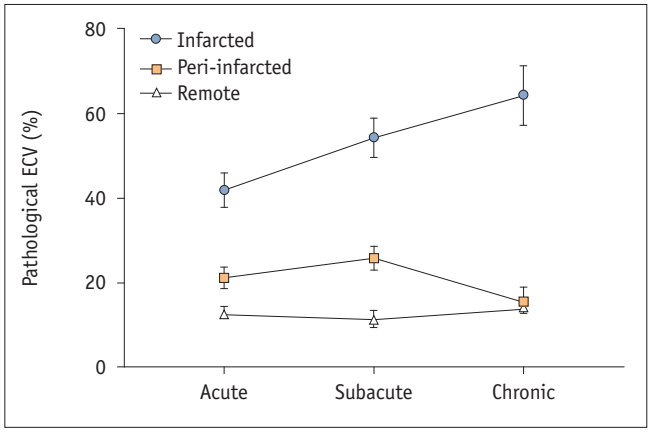

A

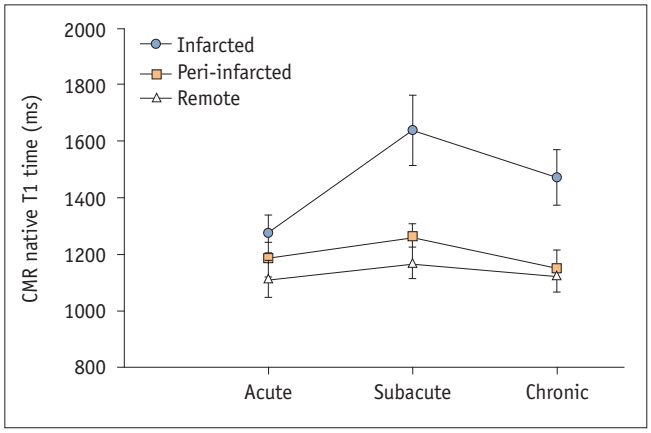

B

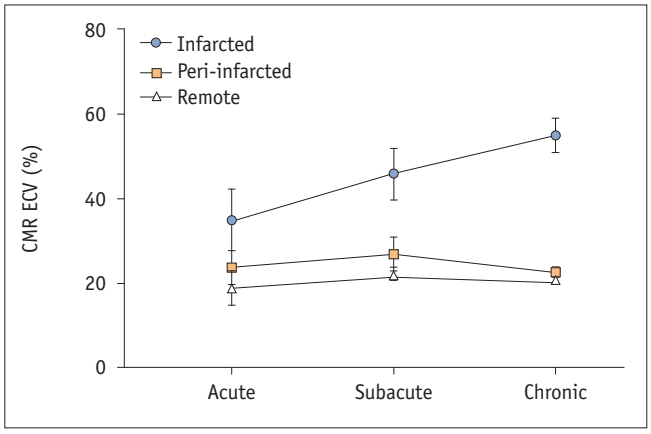

C

Fig. 3. Native T1, CMR-derived ECV, and pathological findings varied with time in different severity of myocardium injury. **A.** The histological ECV showed a trend in infarcted and peri-infarcted myocardium, similar to the results of CMR-based ECV. **B.** Infarcted native T1 reached a peak value at the subacute phase. **C.** Infarcted ECV progressively increased with time.

Native T1 mapping and ECV measurements have accurate performance in the quantitative evaluation of myocardial injury after MI (8, 18). These findings are explained by the results from our analysis of mean native T1 and ECV in different areas of the myocardium, which in our study were investigated by serial cardiac MR scans of pig models in the acute, subacute and chronic stages. Our data showed that from remote to infarcted myocardium, the progressive elevation occurred in both native T1 and ECV in acute and subacute phases, which is consistent with the data of previous study demonstrating myocardial blood flow was worst in infarcted myocardium (8). In the chronic stage, we found no difference in the two parameters between the peri-infarct and remote myocardium, which indicates the resorption of edema and tissue healing occurring in the adjacent to the infarcted zone. Additionally, our results are agreement with the findings in published literature reporting higher native T1 and ECV in infarcted myocardium compared with remote myocardium (23, 24).

From acute to chronic study, native T1 of infarcted myocardium showed a wave-like trend with a peak value in the subacute phase. This trend is similar to the new perspective (25-27) that myocardial edema presents a bimodal phenomenon post-infarction, although the current study was not performed at earlier imaging times. The peak value of infarcted native T1 might indicate severe myocardial edema after the first week in MI because of the inflammation response and tissue healing-related granulation developing (27). Interestingly, ECV of the infarcted myocardium showed a different trend as progressive elevation. ECV allows the measurement of extracellular space expansion and appears as a quantitative map due to gadolinium being trapped in the significant expanded extracellular space and intra-cell through the raptured membrane and capillaries after acute MI. As myocardial edema resolved after MI, already damaged cells were increasingly replaced by extensive collagenous deposition with time (27), leading to an increase in gadolinium concentration (28). Several researches have demonstrated that ECV could serve as a reliable quantitative marker of myocardial fibrosis (29, 30). Thus, the observed progressive ECV elevation over time potentially suggests

https://doi.org/10.3348/kjr.2020.0107

Korean Journal of Radiology
KJR

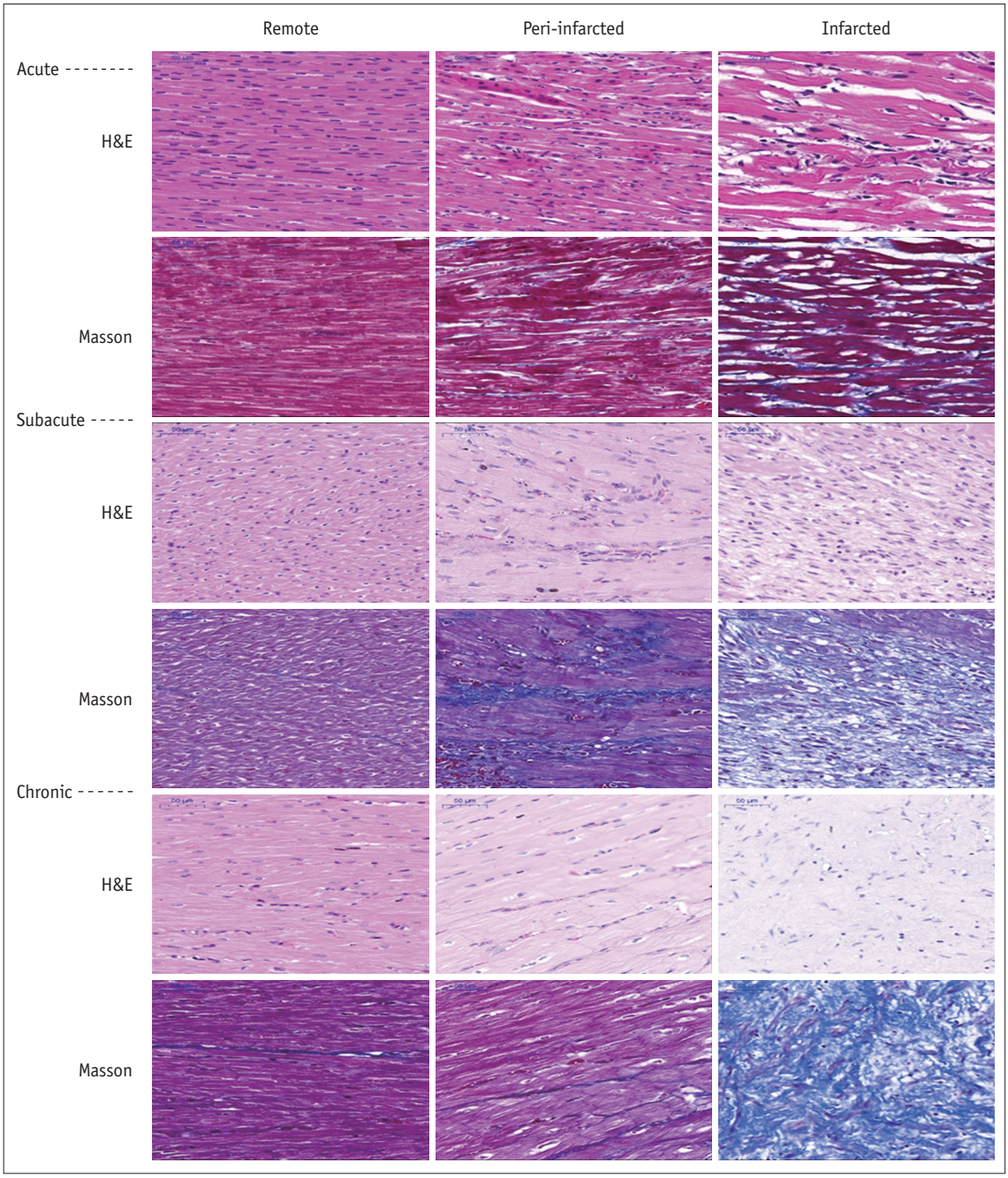

Fig. 4. Representative sections from three areas of the myocardium: remote myocardium, peri-infarcted myocardium, and infarcted myocardium (magnification, x 200). H&E staining showed myocytolysis, inflammatory cell recruitment, and intracellular and extracellular edema in acutely infarcted myocardium. The inflammation and edema of the infarcted myocardium gradually released over time. On the other hand, Masson staining (red = myocardial cells) demonstrated the progressive deposition of collagen and increased ECV in infarcted myocardium with a longer duration of ischemia. H&E = hematoxylin and eosin

that myocardial fibrosis became increasingly severe in the infarcted myocardium, which is in line with the exacerbating in fibrous deposition observed in our histological study.

The occurrence of MVO has different influences on native T1 and ECV. Native T1 increased due to tissue edema by activation of inflammatory reactions in the area of MVO (31). On the contrary, the blood degradation products, such as deoxyhemoglobin, could prolong T1 relaxation time, resulting in a lower native T1 compared to the infarcted myocardium without MVO. As for the influence of MVO on ECV, the microvasculature surrounding MVO is morphological intact, severe disruption of endothelial cells and

https://doi.org/10.3348/kjr.2020.0107

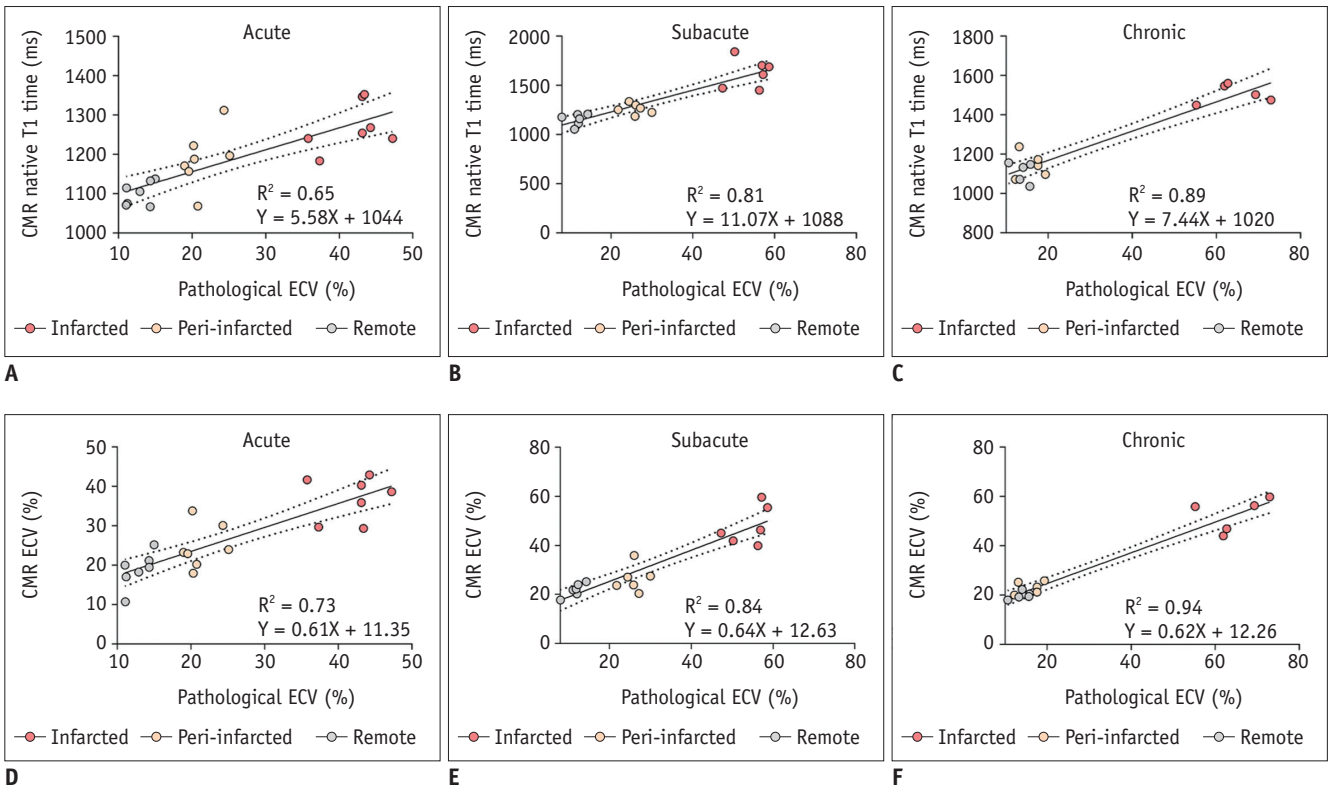

Fig. 5. Correlation between T1 mapping (native T1 and ECV) and histological ECV at three time-points. Both native T1 and ECV correlated well with histological ECV at each imaging time point.

microthrombi occur in the area of microvascular injury (32), leading to an inability of LGE penetrating. This mechanism might result in the failure measurement of true ECV value for MVO.

For MI modeling, pigs are more preferable than dogs due to the close similarities of the anatomical distribution of collateral circulation between the hearts of pigs and humans (33, 34). The islands and peninsulas pattern of necrosis at the edge of infarction yield the lateral extension of salvaged myocardium (6), which is also seen in humans (12, 13). The infarct size showed an apparent reduction in the first week after MI, consistent with previous reports (6, 35) that LGE imaging might overestimate early infarct size in a pig model due to the resolution of edema at the edge of the infarcted region. The slight reduction of infarct size even seen in the subsequent imaging could be explained by the further infarct "shrinkage" (36). However, the ECV of infarcted myocardium increased progressively. Presumably, the myocardial injury is progressive though the infarct size is reducing after MI.

Histological features in MI are complex and dynamic changes over time (27, 36). Thus, an appropriate strategy is needed to monitor the evolution of myocardium injury which plays a key role in clinical therapy decision and prognosis prediction. Numerous studies have provided robust evidence that native T1 and ECV are susceptible to varying degrees of myocardial edema (11, 37) and collagenous fibrosis (38). The different trends between native T1 and ECV and the strong correlation compared with histological findings observed in the study suggest that native T1 mapping is more sensitive to edematous assessment, while ECV measurement is more helpful in the quantification of myocardial fibrosis in MI. Furthermore, these data are a reminder of the importance of appropriate time points for evaluating myocardial injury progression using T1 mapping parameters.

Limitations

The current study has several limitations. First, the native T1 and ECV of different degrees of severity of injured myocardium were measured by manually drawing ROIs, which are subject to the influence of subjective judgment. Despite this drawback, this measurement is widely used in existing clinical practice. Furthermore, the experimental study did not set up the baseline examination of the same pig. However, the pig cohorts were imaged at three-time

https://doi.org/10.3348/kjr.2020.0107

Korean Journal of Radiology
KJR

points for monitoring the dynamic changes of myocardial injury after MI. Additionally, in this study, we did not assess post-T1 values because this index easily affects various factors during CMR examination (39, 40).

Conclusion

In conclusion, we successfully imaged and quantified the different severities of damaged myocardium using native T1 and ECV maps. These results indicated that T1 mapping could provide a noninvasive and robust means to assess and monitor the myocardial injury evolution post-infarction.

Conflicts of Interest

The authors have no potential conflicts of interest to disclose.

ORCID iDs

Lu Zhang
https://orcid.org/0000-0002-0307-7113
Zhi-gang Yang
https://orcid.org/0000-0001-9341-7697
Huayan Xu
https://orcid.org/0000-0001-7276-6142
Meng-xi Yang
https://orcid.org/0000-0001-9780-3536
Rong Xu
https://orcid.org/0000-0001-5974-1258
Lin Chen
https://orcid.org/0000-0002-2093-1801
Ran Sun
https://orcid.org/0000-0003-2621-2733
Tianyu Miao
https://orcid.org/0000-0002-3762-7937
Jichun Zhao
https://orcid.org/0000-0002-8846-682X
Xiaoyue Zhou
https://orcid.org/0000-0002-7094-4731
Chuan Fu
https://orcid.org/0000-0001-9737-0806
Yingkun Guo
https://orcid.org/0000-0001-8437-9887

REFERENCES

1. Nabel EG, Braunwald E. A tale of coronary artery disease and myocardial infarction. *N Engl J Med* 2012;366:54-63
2. Ezekowitz JA, Kaul P, Bakal JA, Armstrong PW, Welsh RC, McAlister FA. Declining in-hospital mortality and increasing heart failure incidence in elderly patients with first myocardial infarction. *J Am Coll Cardiol* 2009;53:13-20
3. Carrick D, Haig C, Rauhalammi S, Ahmed N, Mordi I, McEntegart M, et al. Prognostic significance of infarct core pathology revealed by quantitative non-contrast in comparison with contrast cardiac magnetic resonance imaging in reperfused ST-elevation myocardial infarction survivors. *Eur Heart J* 2016;37:1044-1059
4. Wu E, Ortiz JT, Tejedor P, Lee DC, Bucciarelli-Ducci C, Kansal P, et al. Infarct size by contrast enhanced cardiac magnetic resonance is a stronger predictor of outcomes than left ventricular ejection fraction or end-systolic volume index: prospective cohort study. *Heart* 2008;94:730-736
5. van Kranenburg M, Magro M, Thiele H, de Waha S, Eitel I, Cochet A, et al. Prognostic value of microvascular obstruction and infarct size, as measured by CMR in STEMI patients. *JACC Cardiovasc Imaging* 2014;7:930-939
6. Jablonowski R, Engblom H, Kanski M, Nordlund D, Koul S, van der Pals J, et al. Contrast-enhanced CMR overestimates early myocardial infarct size: mechanistic insights using ECV measurements on day 1 and day 7. *JACC Cardiovasc Imaging* 2015;8:1379-1389
7. Dall'Armellina E, Karia N, Lindsay AC, Karamitsos TD, Ferreira V, Robson MD, et al. Dynamic changes of edema and late gadolinium enhancement after acute myocardial infarction and their relationship to functional recovery and salvage index. *Circ Cardiovasc Imaging* 2011;4:228-236
8. Liu D, Borlotti A, Viliani D, Jerosch-Herold M, Alkhalil M, De Maria GL, et al. CMR native T1 mapping allows differentiation of reversible versus irreversible myocardial damage in ST-segment-elevation myocardial infarction: an OxAMI Study (Oxford Acute Myocardial Infarction). *Circ Cardiovasc Imaging* 2017;10:e005986
9. Messroghli DR, Walters K, Plein S, Sparrow P, Friedrich MG, Ridgway JP, et al. Myocardial T1 mapping: application to patients with acute and chronic myocardial infarction. *Magn Reson Med* 2007;58:34-40
10. Kali A, Choi EY, Sharif B, Kim YJ, Bi X, Spottiswoode B, et al. Native T1 mapping by 3-T CMR imaging for characterization of chronic myocardial infarctions. *JACC Cardiovasc Imaging* 2015;8:1019-1030
11. Tahir E, Sinn M, Bohnen S, Avanesov M, Säring D, Stehning C, et al. Acute versus chronic myocardial infarction: diagnostic accuracy of quantitative native T1 and T2 mapping versus assessment of edema on standard T2-weighted cardiovascular MR images for differentiation. *Radiology* 2017;285:83-91
12. Ugander M, Bagi PS, Oki AJ, Chen B, Hsu LY, Aletras AH, et al. Myocardial edema as detected by pre-contrast T1 and T2 CMR delineates area at risk associated with acute myocardial infarction. *JACC Cardiovasc Imaging* 2012;5:596-603
13. Garg P, Broadbent DA, Swoboda PP, Foley JRJ, Fent GJ, Musa TA, et al. Acute infarct extracellular volume mapping to quantify myocardial area at risk and chronic infarct size on

 https://doi.org/10.3348/kjr.2020.0107

cardiovascular magnetic resonance imaging. *Circ Cardiovasc Imaging* 2017;10:e006182
14. Ugander M, Oki AJ, Hsu LY, Kellman P, Greiser A, Aletras AH, et al. Extracellular volume imaging by magnetic resonance imaging provides insights into overt and sub-clinical myocardial pathology. *Eur Heart J* 2012;33:1268-1278
15. Sibley CT, Noureldin RA, Gai N, Nacif MS, Liu S, Turkbey EB, et al. T1 mapping in cardiomyopathy at cardiac MR: comparison with endomyocardial biopsy. *Radiology* 2012;265:724-732
16. Iles LM, Ellims AH, Llewellyn H, Hare JL, Kaye DM, McLean CA, et al. Histological validation of cardiac magnetic resonance analysis of regional and diffuse interstitial myocardial fibrosis. *Eur Heart J Cardiovasc Imaging* 2015;16:14-22
17. Shiina Y, Inai K, Taniguchi K, Takahashi T, Nagao M. Potential value of native T1 mapping in symptomatic adults with congenital heart disease: a preliminary study of 3.0 tesla cardiac magnetic resonance imaging. *Pediatr Cardiol* 2020;41:94-100
18. Dall'Armellina E, Piechnik SK, Ferreira VM, Si QL, Robson MD, Francis JM, et al. Cardiovascular magnetic resonance by non contrast T1-mapping allows assessment of severity of injury in acute myocardial infarction. *J Cardiovasc Magn Reson* 2012;14:15
19. Schulz-Menger J, Bluemke DA, Bremerich J, Flamm SD, Fogel MA, Friedrich MG, et al. Standardized image interpretation and post processing in cardiovascular magnetic resonance: Society for Cardiovascular Magnetic Resonance (SCMR) board of trustees task force on standardized post processing. *J Cardiovasc Magn Reson* 2013;15:35
20. Bondarenko O, Beek AM, Hofman MB, Kühl HP, Twisk JW, van Dockum WG, et al. Standardizing the definition of hyperenhancement in the quantitative assessment of infarct size and myocardial viability using delayed contrast-enhanced CMR. *J Cardiovasc Magn Reson* 2005;7:481-485
21. Heiberg E, Ugander M, Engblom H, Götberg M, Olivecrona GK, Erlinge D, et al. Automated quantification of myocardial infarction from MR images by accounting for partial volume effects: animal, phantom, and human study. *Radiology* 2008;246:581-588
22. Arheden H, Saeed M, Higgins CB, Gao DW, Bremerich J, Wyttenbach R, et al. Measurement of the distribution volume of gadopentetate dimeglumine at echo-planar MR imaging to quantify myocardial infarction: comparison with 99mTc-DTPA autoradiography in rats. *Radiology* 1999;211:698-708
23. Lee SP, Lee W, Lee JM, Park EA, Kim HK, Kim YJ, et al. Assessment of diffuse myocardial fibrosis by using MR imaging in asymptomatic patients with aortic stenosis. *Radiology* 2015;274:359-369
24. de Meester de Ravenstein C, Bouzin C, Lazam S, Boulif J, Amzulescu M, Melchior J, et al. Histological validation of measurement of diffuse interstitial myocardial fibrosis by myocardial extravascular volume fraction from modified Look-Locker imaging (MOLLI) T1 mapping at 3 T. *J Cardiovasc Magn Reson* 2015;17:48
25. Fernández-Jiménez R, Barreiro-Pérez M, Martin-García A, Sánchez-González J, Agüero J, Galán-Arriola C, et al. Dynamic edematous response of the human heart to myocardial infarction: implications for assessing myocardial area at risk and salvage. *Circulation* 2017;136:1288-1300
26. Fernández-Jiménez R, Sánchez-González J, Agüero J, García-Prieto J, López-Martín GJ, García-Ruiz JM, et al. Myocardial edema after ischemia/reperfusion is not stable and follows a bimodal pattern: imaging and histological tissue characterization. *J Am Coll Cardiol* 2015;65:315-323
27. Fernández-Jiménez R, García-Prieto J, Sánchez-González J, Agüero J, López-Martín GJ, Galán-Arriola C, et al. Pathophysiology underlying the bimodal edema phenomenon after myocardial ischemia/reperfusion. *J Am Coll Cardiol* 2015;66:816-828
28. Klein C, Nekolla SG, Balbach T, Schnackenburg B, Nagel E, Fleck E, et al. The influence of myocardial blood flow and volume of distribution on late Gd-DTPA kinetics in ischemic heart failure. *J Magn Reson Imaging* 2004;20:588-593
29. Messroghli DR, Moon JC, Ferreira VM, Grosse-Wortmann L, He T, Kellman P, et al. Clinical recommendations for cardiovascular magnetic resonance mapping of T1, T2, T2* and extracellular volume: a consensus statement by the Society for Cardiovascular Magnetic Resonance (SCMR) endorsed by the European Association for Cardiovascular Imaging (EACVI). *J Cardiovasc Magn Reson* 2017;19:75
30. Messroghli DR, Nordmeyer S, Dietrich T, Dirsch O, Kaschina E, Savvatis K, et al. Assessment of diffuse myocardial fibrosis in rats using small-animal Look-Locker inversion recovery T1 mapping. *Circ Cardiovasc Imaging* 2011;4:636-640
31. van der Laan AM, Piek JJ, van Royen N. Targeting angiogenesis to restore the microcirculation after reperfused MI. *Nat Rev Cardiol* 2009;6:515-523
32. Robbers LF, Eerenberg ES, Teunissen PF, Jansen MF, Hollander MR, Horrevoets AJ, et al. Magnetic resonance imaging-defined areas of microvascular obstruction after acute myocardial infarction represent microvascular destruction and haemorrhage. *Eur Heart J* 2013;34:2346-2353
33. Ngai JH, Matlib MA, Millard RW. Contractile performance, mitochondrial function and blood flow distribution in porcine heart with induced coronary collateral circulation. *Basic Res Cardiol* 1983;78:62-76
34. Bøtker HE, Hausenloy D, Andreadou I, Antonucci S, Boengler K, Davidson SM, et al. Practical guidelines for rigor and reproducibility in preclinical and clinical studies on cardioprotection. *Basic Res Cardiol* 2018;113:39
35. Ibrahim T, Hackl T, Nekolla SG, Breuer M, Feldmair M, Schömig A, et al. Acute myocardial infarction: serial cardiac MR imaging shows a decrease in delayed enhancement of the myocardium during the 1st week after reperfusion. *Radiology* 2010;254:88-97
36. Ibanez B, Aletras AH, Arai AE, Arheden H, Bax J, Berry C, et al. Cardiac MRI endpoints in myocardial infarction experimental and clinical trials: JACC scientific expert panel.

https://doi.org/10.3348/kjr.2020.0107

J Am Coll Cardiol 2019;74:238-256
37. Williams ES, Kaplan JI, Thatcher F, Zimmerman G, Knoebel SB. Prolongation of proton spin lattice relaxation times in regionally ischemic tissue from dog hearts. *J Nucl Med* 1980;21:449-453
38. Bull S, White SK, Piechnik SK, Flett AS, Ferreira VM, Loudon M, et al. Human non-contrast T1 values and correlation with histology in diffuse fibrosis. *Heart* 2013;99:932-937
39. Gai N, Turkbey EB, Nazarian S, van der Geest RJ, Liu CY, Lima JA, et al. T1 mapping of the gadolinium-enhanced myocardium: adjustment for factors affecting interpatient comparison. *Magn Reson Med* 2011;65:1407-1415
40. Mewton N, Liu CY, Croisille P, Bluemke D, Lima JA. Assessment of myocardial fibrosis with cardiovascular magnetic resonance. *J Am Coll Cardiol* 2011;57:891-903

 https://doi.org/10.3348/kjr.2020.0107